Experimental characterization of active and nonactive harmonic power flow of AC rolling stock and interaction with the supply network

Andrea Mariscotti

This file is the pre-print version of:
A. Mariscotti, "Experimental characterization of active and nonactive harmonic power flow of AC rolling stock and interaction with the supply network," *IET Electrical Systems in Transportation*, 2021, in print.

Experimental characterization of active and nonactive harmonic power flow of AC rolling stock and interaction with the supply network

Andrea Mariscotti

DITEN, University of Genova, Via Opera Pia 11A, Genova, Italy
*andrea.mariscotti@unige.it

Abstract: In AC electrified railways there is a significant exchange of power at fundamental and harmonics in quite dynamic conditions. Harmonic patterns of AC rolling stock and railway networks are analysed in terms of active and nonactive power flow, relating it to the characteristic of the network and to operating conditions, synthesized in the fundamental current intensity and speed. The work shows that correlation and clustering can separate distortion terms of internal and external origin also without a priori information. The use of harmonic power terms (product of voltage and current components) shows improved robustness with respect to the analysis of the voltage and current components alone.

1. Introduction

It is generally recognized that reactive power and harmonic distortion are responsible for increased losses in the feeding system, from which the many regulatory standards, especially for public and industrial networks [1][2]. Considering ac railways, besides relevant nonactive power terms, it was demonstrated in [3]-[5] that some harmonics can contribute to the active power flow. This is confirmed for variable speed drives [6]-[10], which are the main harmonic source onboard. Auxiliary onboard converters are also a relevant source, especially because of higher distortion (e.g. diode rectifier front end), visible in low traction effort conditions.

Rolling stock harmonic emissions are assessed and analyzed for a variety of purposes: first of all prevention of interference to signalling, directly conducted or by induction [11][12] and more recently for assessment of power and energy consumption [3]-[5][13], all carried out in a single-train perspective. Thus information on network and its quantities is limited to what can be measured at the line-pantograph interface. This may be seen as a restriction compared to other industrial applications, which see several interconnected Power Measurement Units and significant efforts to model and identify network response and propagation, especially for smart grids [14][15]. It is noted that an electrified railway is a continuously changing network with moving loads in quite dynamic conditions, and that the single-point measurement approach suites the vast range of rolling stock from different operators and manufacturers travelling within it. A metro conversely is an application with a known fleet that moves in a defined and delimited environment; partially networked solutions might be implemented e.g. at the Automatic Train Operation level. Metros are generally singly owned and accounting and fair billing are then purely formal. In addition, metros are dc supplied, with less relevant harmonic power terms, as confirmed by the preliminary analysis in [3].

The technological progress in the field of power conversion offers faster, lighter, more compact and more efficient converters with emissions spread farther over the frequency axis. At the same time electric transportation will reduce headway, packing more densely vehicles and trains, featuring faster and smarter dynamics. Smart and micro grids have anticipated this tendency: supraharmonics have come into play beyond the "usual" harmonics [16][17], with issues of network resonance also for small-size networks. Railways feature resonance at lower frequency, relevant for induction, interference and voltage stability [11][12][18]-[20]. Besides resonance, traction current harmonics undergo a significant phase rotation, indicating diversified propagation and interaction between vehicles [21]. In general, the harmonic spectrum of a vehicle in a real traffic scenario will feature components of internal and external origin, where the onboard power circuit behave as a nonlinear distorting circuit or simply as a passive load.

Focusing on the significance of harmonic power and its impact on energy consumption and its metering, it is observed that the target uncertainty of EN 50463-2 [13] is a fraction of %, and it was demonstrated that harmonics altogether can bring a fraction of the fundamental active power of the same order [3]-[5], and that the harmonic nonactive power is much larger. This means that the amplitude of harmonic power terms and their variability during train operation are a relevant factor for the uncertainty budget of the power and energy consumption. Although it is true that rolling stock input distortion is at all affected by the system timetable, when an optimization strategy changes intervals of traction, coasting, cruising and braking, correspondingly harmonic patterns and harmonic power will change, shifting in time or space along the line.

The analysis is carried out with experimental data collected in a single-train perspective [22].

2. Power quantities definition

Power quantities are introduced using IEEE Std. 1459 [23]. The total apparent power in nonsinusoidal conditions results from the multiplication of the two vectors of voltage and current at the pantograph, expressed as vectors of harmonic components: the order h is referred to fundamental pulsation ω, V_h and I_h are the amplitudes and α_h and β_h the phases of the h-th voltage and current component, respectively.

$$v_p = V_0 + \sqrt{2}\sum_h V_h \sin(h\omega t - \alpha_h) \quad (1a)$$

$$i_p = I_0 + \sqrt{2}\sum_h I_h \sin(h\omega t - \beta_h) \quad (1b)$$

Active and nonactive power terms may be conveniently separated as in [24][25]:

- active power terms for the fundamental P_1 and harmonics P_h (resulting from the product of voltage and current components of the same order) are shown in (2);
- nonactive power terms, encompassing reactive and distortion terms, resulting from multiplication of harmonics of different order and the fundamental or dc component (that for ac railways may be neglected), as in (3).

$$p_a = \sum_h V_h I_h \cos\vartheta_h [1 - \cos(2h\omega t - 2\alpha_h)] \quad (2)$$

$$\begin{aligned} p_q = &- \sum_h V_h I_h \sin\vartheta_h \sin(2h\omega t - 2\alpha_h) \\ &+ 2\sum_m \sum_{m\neq n} V_m I_n \sin(m\omega t - \alpha_m)\sin(n\omega t - \beta_n) \\ &+ V_0 \sum_h I_h \sin(h\omega t - \beta_h) + I_0 \sum_h V_h \sin(h\omega t - \alpha_h) \end{aligned} \quad (3)$$

where:

- the first term is the harmonic reactive power Q_h;
- the second term is a set of mixed products defining the distortion power D_h and involving both fundamental and harmonics; this term differes from that defined in IEEE Std. 1459 (D_H), that includes Q_h.

The objective is the characterization of active and nonactive power in terms of amplitude and distribution, compared to the fundamental terms:

- Active power terms at fundamental and harmonics can be summed, all contributing to the total active power

$$P_t = P_1 + \Sigma P_h \quad (4)$$

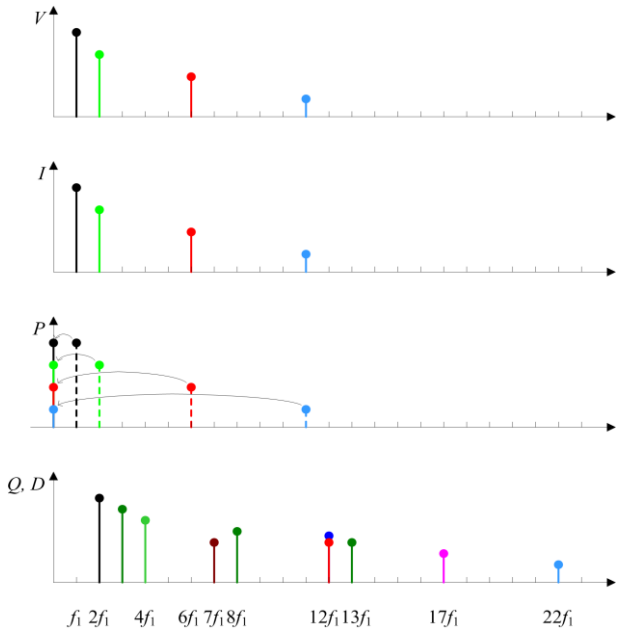

Fig. 1. Active and nonactive power components resulting from the combination of voltage and current harmonics.

- Nonactive power terms should be considered in terms of absolute value, to indicate the amount of exchanged power; reactive Q and distortion D power terms can then be summed together to get the total nonactive power N_t. N_t may be determined as quadratic difference of total apparent power S_t=$V_{rms}I_{rms}$ and total active power P_t. N_t corresponds to the Fryze's fictitious power:

$$N_t = \sqrt{S_t^2 - P_t^2} \quad (5)$$

An example with a fundamental and three harmonics (total n=4) for both the voltage and the current vectors is shown in Fig. 1, using colours and height to suggest the pairing of components to give the nonactive power terms: it is immediate that their number increases significantly with n (as $n + n(n-1)/2$, with the "/2" accounting for duplicated terms due to symmetry of the multiplication).

3. Rolling Stock and Network data

Trains are characterized by harmonic patterns caused by the various non-linear loads on-board: waveform distortion and thus harmonic amplitude and distribution are different depending on the operating conditions. Differences may be observed e.g. between traction and braking (occurring through the same four-quadrant converters, 4QCs, in ac rolling stock) or during coasting and at standstill (when distortion is increased by the contribution of auxiliaries). For both situations normative requirements to limit harmonics are still not fully addressing the problem: the EN 50388 [26] focuses only on the fundamental to define the "power factor", although the prEN 50388-1 (draft of 2017, [27]) clearly separates the displacement factor from the power factor, the latter correctly including harmonics, but no limits are given, indicating the need for a compatibility study.

Partial cancellation of some components is in principle possible in the presence of more than one instance of the same model of rolling stock: not such an uncommon scenario, if we consider that regional and commuter trains of the same operator are probably pulled by the same type of locomotive, as well as a fleet of high-speed trains is composed by lots of few different models. The harmonic components from the rolling stock undergo phase rotation whilst propagating along the traction line [21], overlapping within the same supply section, that for a 16.7 Hz system may be quite long, whereas in general for 50 Hz systems is limited to about 30-50 km.

Pantograph voltage and current waveforms (v_p and i_p) sampled and arranged in a dataset [22] with tags to indicate overall power absorption and speed as overall indication of rolling stock operating conditions, distinguishing traction, braking, coasting and standstill (this colour notation is used in the spectra of Fig. 2: traction in red, braking in blue, coasting in black and standstill in green). Each short record (called "snippet") has duration of five fundamental cycles, keeping harmonics well separated with frequency resolution of one fifth the fundamental: the spectra V_p and I_p of records are calculated using the Discrete Fourier Transform with a window T of 300 ms for the 16.7 Hz and 100 ms for the 50 Hz system. The selected time window is in line with the fastest time step adopted for electromechanical simulation

[28][29], indicating that an almost steady-state assumption may be made for train kinematics and mechanical quantities. The snippets were extracted from continuous recordings every 2 seconds. The original data were sampled at 50 kS/s, ensuring sufficient oversampling even at the highest harmonics covered by this analysis, set to 5 kHz in agreement with previous works [3]-[5]. Each window T is transformed using a Hann window for spectral leakage.

The data refer to the following trains and networks:

- Switzerland: Romanshorn – Zurich – Brig with a Re460 locomotive (5.6 MW nominal power) in normal service; the switching frequency of the 4QC traction converter is 800 Hz resulting from four interleaved GTO converters each with 200 Hz switching frequency;
- Germany: Hamburg – Dortmund – Frankfurt with ICE-S train during test runs, whose power drive is similar to that of the ICE2, so based on GTO technology;
- France: Paris – Lyon with a TGV Dasye EMU (9.28 MW total nominal power) during test runs; the power chain of TGV Duplex series has diode rectifiers featuring a GTO power factor control and thyristors inverters.

The typical V_p and I_p spectra are shown in Fig. 2 as a reference for the discussion of the power indexes in sec. 4 and for the interpretation of results in sec. 5.

Both systems feature a prevalent distortion on odd harmonics, with the exception of significant, but dispersed, values on the 2nd and 4th harmonic. The 3rd voltage harmonic is significant in all systems with different corresponding current intensity, depending e.g. on the rolling stock input impedance. For France the amplitude of harmonics is consistently above or close to 1000 Vrms up to about 2000 Hz, about 3 times larger than 16.7 Hz systems, once weighted by the respective nominal voltages [30]; also the 2nd harm. is larger and more dispersed, peaking occasionally (about 5% of time) to relevant values. The current spectrum for the Swiss case shows a consistent presence of loco harmonic signature between the 37th (617 Hz) and the 59th (983 Hz) harmonics. Other components at 2000 Hz are known to be due to other trains on the same line section, and possibly the components at about 1300 Hz. Similarly for Germany there are about five recognizable harmonic clusters at about 700, 1100, 1350, 1650 and 2000 Hz. For France the recognizable harmonic clusters are at 1750, 2500 and 4000 Hz; the peak at 4850 Hz visible particularly in the

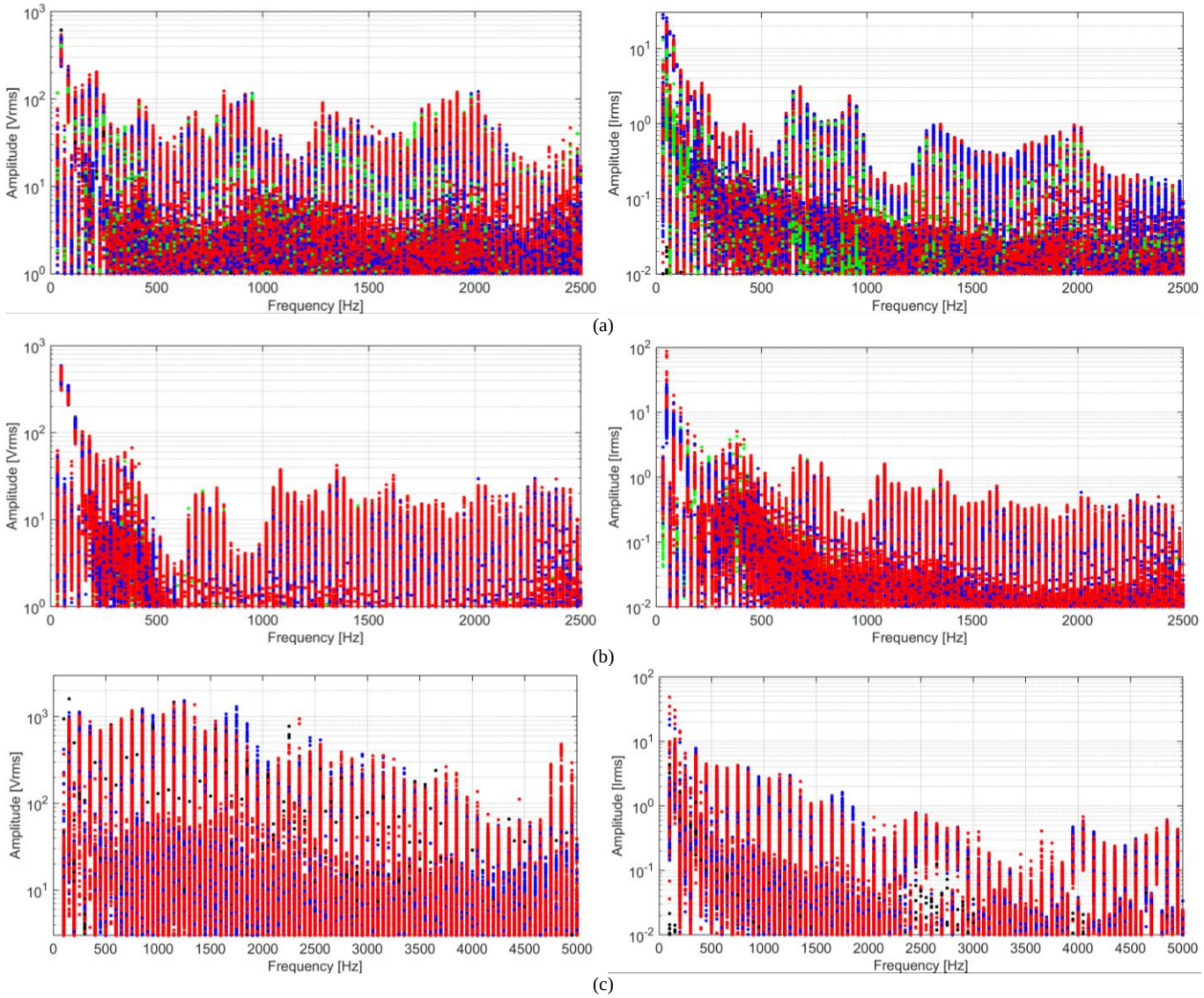

Fig. 2. Harmonic spectrum of V_p and I_p (traction in red, braking in blue, coasting in black and standstill in green): ***(a)*** *16.7 Hz system (Switzerland),* ***(b)*** *16.7 Hz system (Germany),* ***(c)*** *50 Hz system (France)*

voltage spectrum may be the result of voltage amplification due to line resonance [18]-[20].

4. Power flow indexes

4.1. Basic quantities

Harmonic power terms can be evaluated and analyzed by defining suitable basic indexes that focus on a single component using the framework set forth in sec. 2. A combination of power components normalized by overall power terms is considered in the following.

As shown in sec. 2 and Fig. 1, each harmonic has a clearly defined active power P_h and reactive power Q_h (at twice the frequency), whereas the distortion power terms are related to pairs of components (m and n, including fundamental and harmonics). Invoking (3) half of each D_{mn} term may be assigned to each one of the two components m and n of the pair, although it is difficult to apply this rule when the fundamental is involved (m=1), because the new D_{mn} term would add to the existing Q_1, modifying the definition of the nonactive power at the fundamental from "reactive" only to "reactive + distortion". For this reason it is opted to assign the resulting D_{1n} only to the harmonic n. For the interpretation of Q_h opinions are mixed, maintaining that isolating Q_h from the nonactive harmonic power is groundless: without discussing it, we simply state that isolating Q_h is convenient to define the harmonic power displacement factor $d_h = P_h/S_h + j\, Q_h/S_h$.

The simple harmonic active power P_h well describes the flow of energy into and from the rolling stock, and may be considered a valid index, as discussed in [25], together with various distortion power indexes as single-point harmonic producer indicators. Active and nonactive power terms may be also displayed as a fraction of the respective fundamental quantities or of the global values, as used in [3].

4.2. Enhanced representations

Elaborations of basic indexes are considered to identify, visualize and track the harmonic signature of rolling stock, separating its harmonic components from those related to other rolling stock items and in general network distortion.

The harmonic active power flow P_h, also named Active Power Indicator [25], is quite useful to identify harmonics involved in the transfer of energy: both its statistics (e.g. percentiles) and the direction of flow (sign of P_h) are effective to display and track distortion power.

The introduced power displacement factor d_h or better the pair P_h-Q_h (in order to include the information of intensity) can be displayed in polar coordinates and lend themselves to clustering and separation of operating modes.

Similarly, V_h and I_h plotted in a Lissajous diagram give the amplitude of a complex quantity, the instantaneous impedance, $\xi_h = V_h/I_h$, with similar approach but less robust to noise and local variations.

The power quantities discussed in sec. 2 can all be evaluated using correlation and similarity with quantities taken to represent the operating conditions: in the present case the rms of I_p, *Irms* (a nonnegative quantity), or the fundamental I_1 (including rms information and sign), and the speed s.

P_h-Q_h and V_h-I_h diagrams lend themselves to visual interpretation, evaluating the degree of clustering between different operating conditions (o.c.) and time intervals (t.i.): for a consistent relationship with a specific o.c., it is expected that the cluster shape repeats in different t.i.. External sources are expected to be uncorrelated and change within the same o.c., although it must be noted that the input impedance of the rolling stock is in general lower during traction, so a slight amplification of current components (and thus of power terms) of external origin is expected. Criteria are clarified with the examples of the next section.

5. Results for 16.7 Hz and 50 Hz systems

The experimental data of the 16.7 and 50 Hz systems are used to analyse and discuss the characteristics of the identified quantities and representations.

5.1. Active Power flow

The largest harmonic active power P_h components are plotted in Fig. 3 and Fig. 4 for the 16.7 Hz systems, considering time intervals with traction, braking and coasting phases. The sign of P_h , $\underline{P_h}$, is shown in red when directed into the loco, in blue when to the outside of it.

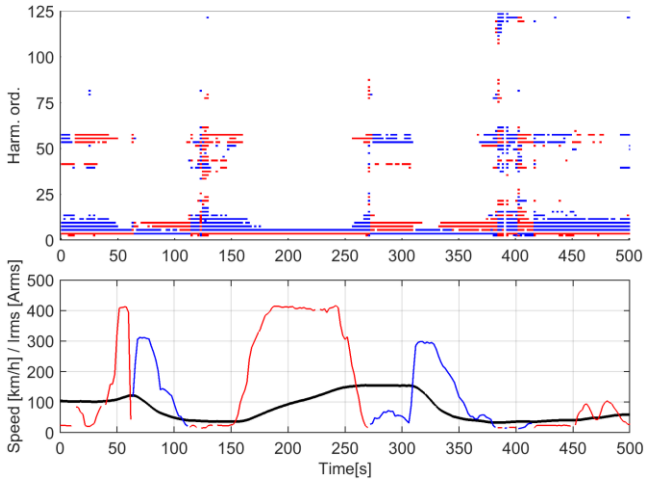

Fig. 3. Distribution of largest P_h values (98% percentile) and relation of $\underline{P_h}$ with speed (black) and Irms for the Swiss 16.7 Hz system (traction=red, braking=blue).

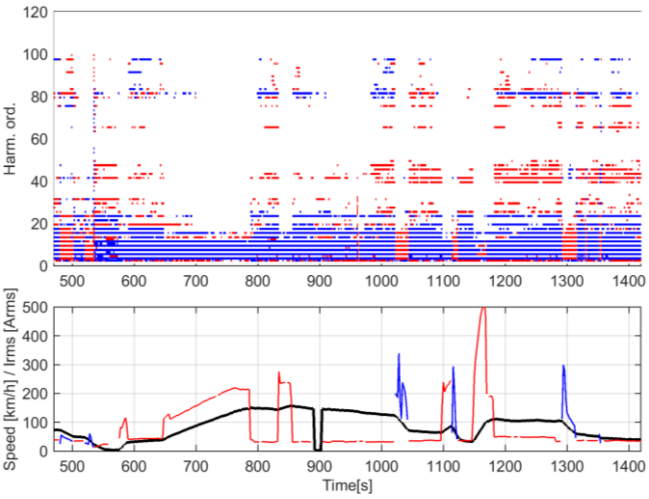

Fig. 4. Distribution of largest P_h values (95% percentile) and relation of $\underline{P_h}$ with speed (black) and Irms for the German 16.7 Hz system (traction=red, braking=blue).

In Fig. 3 we may observe that the 2nd harmonic pulls significant active power almost in correspondence of blank intervals of very small *Irms* values, characterized by very large distortion, and for this reason discarded from the traction/braking classification. The 3rd harmonic pulls or pushes active power almost synchronized with traction and braking. The 3rd harmonic is influenced by different factors: it is a network voltage harmonic and it is a by-product of the difficulty of following the sinusoidal reference with a low switching frequency of the 4QC [9], but it is also the fundamental frequency for auxiliaries, operating at 50 Hz, not at the traction frequency of 16.7 Hz. Also the 5th and 7th are synchronized, but with opposite behaviour: harmonic active power enters the loco during braking and leaves it during tractioning. The low-order harmonics are in general prevalent; onboard converter harmonics become relevant in low-load conditions during coasting and standstill.

Fig. 4 shows the behaviour of another 16.7 Hz system (Germany), that is different, with more intense low-order harmonics and the 4QC components appearing between the 41st and the 55th harmonic (after having selected the 95% percentile for display purposes). The second 4QC group may be observed around the 80th order, possibly mixed with other contributions. As expected, the P_h relevance for the 4QC terms is higher in time intervals with low traction effort. For low-order harmonics it is peculiar that P_h reverses its sign entering the rolling stock during braking, as already observed for the Swiss system in Fig. 3.

Fig. 5 shows P_h vs. *Irms* and speed for the 50 Hz system.

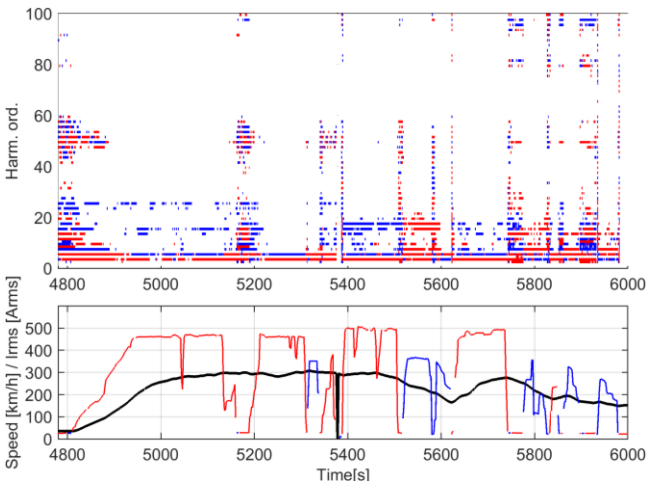

Fig. 5. Distribution of largest P_h values (95% percentile) and relation with speed (black) and Irms for the French 50 Hz system (traction=red, braking=blue).

In Fig. 5 the initial low-speed coasting interval before 4800 s is characterized by low order harmonics up to 25th and higher order harmonics between 45th and 57th. The same repeats for the mixed cruising/coasting at higher speed (300 kmph) that can be observed before 5200 s: it is worth underlying that when passing from cruising to coasting P_h for some of the high order harmonic changes its sign. At full traction there are only a few relevant components, namely the 3rd and 5th. The run contains several transients that the tagging algorithm detected as neither traction nor braking (blank segments of the Irms curve) and that are characterized by a burst of several consecutive components. There are two P_h components (15th and 17th) that appear with variable amplitude related to the 4QC operation. At about 5 kHz what was interpreted as a line resonance is visible, excited by transients and during coasting phases.

5.2. Correlation with traction effort and speed

Since speed and *Irms* curves replicate approximately the concept of traction effort, it is interesting to quantify the correlation with the power flow quantities (P_h and Q_h, and the nonactive power N_t). With low distortion, for the purpose of correlation, *Irms* may be exchanged with I_1: for those quantities that show a sign reversal (P_h and Q_h) the intensity I_1 bears its sign, positive when entering the rolling stock; for N_t it is indicated with the absolute value.

A normalized correlation coefficient ρ is calculated, for which the lower and upper bound values ρ_{LB} and ρ_{UB} are also given for the 95% confidence interval of an assumed Gaussian distribution (see Table 1 to 3 for the Swiss 16.7 Hz system and Table 4 to 6 for the French 50 Hz system).

Table 1 Correlation coefficient of P_h with I_1 and speed s (Swiss 16.7 Hz system)

Harm.	$\rho(I_1)$	$\rho_{LB}(I_1)$	$\rho_{UB}(I_1)$	$\rho(s)$	$\rho_{LB}(s)$	$\rho_{UB}(s)$
2	-0.008	-0.035	0.019	0.017	-0.01	0.044
3	0.495	0.475	0.515	0.445	0.423	0.466
5	-0.867	-0.873	-0.860	-0.284	-0.308	-0.259
7	0.128	0.102	0.155	-0.192	-0.218	-0.166
41	0.054	0.027	0.081	-0.264	-0.289	-0.239
43	-0.003	-0.030	0.024	0.162	0.136	0.188
45	0.107	0.081	0.134	0.067	0.040	0.093
47	0.004	-0.023	0.0311	0.0138	-0.013	0.041
49	0.014	-0.013	0.041	0.061	0.034	0.088
51	0.090	0.063	0.116	0.083	0.056	0.101
53	0.125	0.098	0.151	0.055	0.028	0.081
55	0.214	0.188	0.239	0.033	0.006	0.060
57	0.196	0.170	0.222	0.091	0.064	0.117
77	0.086	0.059	0.112	0.129	0.103	0.156
79	0.031	0.005	0.058	-0.074	-0.101	-0.047
81	-0.095	-0.122	-0.069	-0.057	-0.084	-0.030
119	0.017	-0.009	0.044	0.132	0.106	0.158
121	0.030	0.003	0.056	0.133	0.106	0.159

Table 2 Correlation coefficient of Q_h with I_1 and speed s (Swiss 16.7 Hz system)

Harm.	$\rho(I_1)$	$\rho_{LB}(I_1)$	$\rho_{UB}(I_1)$	$\rho(s)$	$\rho_{LB}(s)$	$\rho_{UB}(s)$
2	0.052	0.026	0.079	0.061	0.034	0.088
3	-0.695	-0.709	-0.681	-0.492	-0.512	-0.472
5	0.061	0.034	0.087	-0.162	-0.188	-0.136
7	0.055	0.028	0.082	-0.063	-0.089	-0.036
41	0.161	0.135	0.187	-0.027	-0.053	0.0002
43	-0.215	-0.241	-0.190	-0.234	-0.259	-0.209
45	-0.122	-0.148	-0.095	-0.262	-0.287	-0.237
47	0.011	-0.016	0.038	-0.214	-0.239	-0.188
49	-0.042	-0.069	-0.015	-0.063	-0.089	-0.036
51	-0.024	-0.051	0.003	-0.074	-0.101	-0.048
53	-0.219	-0.244	-0.193	-0.094	-0.121	-0.068
55	-0.075	-0.102	-0.049	0.109	0.082	0.135
57	-0.201	-0.227	-0.175	-0.115	-0.142	-0.089
77	-0.102	-0.129	-0.076	-0.283	-0.307	-0.258
79	-0.025	-0.052	0.0014	0.0057	-0.021	0.033
81	0.079	0.053	0.106	-0.070	-0.096	-0.043
119	-0.016	-0.043	0.011	-0.086	-0.113	-0.060
121	-0.015	-0.042	0.012	-0.093	-0.119	-0.066

It is interesting to observe the significant correlation of the 5th harm for P_h, rather than for Q_h, supporting the idea that P_h is an effective harmonic power indicator, despite the inconsistency in some cases identified in the past for three-phase systems [24][25]. For Switzerland the consistent value of P_h, although smaller than a widely varying Q_h value, is confirmed in Fig. 6 to 8.

P_h at 4QC frequencies is small and this is also confirmed by a stronger correlation of Q_h for 43rd and 45th components. A stronger correlation is observed for the 53rd, 55th and 57th components that carry both active and reactive power. All these components belong to the 4QC modulation pattern centred on the 48th (800 Hz) after interleaving of four 4QC modules, and deviating up to 150 Hz from it.

The overall distortion in terms of total nonactive power N_t is considered in Table 3: the selection of speed s rather than I_1 is important in boosting the correlation value as the N_t quantity is a nonnegative one, whereas I_1 was selected to replicate the direction of current with sign reversal.

Table 3 Correlation coefficient of N_t with I_1 and speed s (Swiss 16.7 Hz system)

$\rho(\lvert I_1\rvert)$	$\rho_{LB}(\lvert I_1\rvert)$	$\rho_{UB}(\lvert I_1\rvert)$	$\rho(s)$	$\rho_{LB}(s)$	$\rho_{UB}(s)$
0.237	0.211	0.262	0.316	0.292	0.340

Table 3 confirms that the nonactive harmonic power N_t is related to the traction/braking effort, higher for larger intensity of the fundamental, although the relationship is not proportional and higher N_t percentages are observed at low current intensity (the correlation coefficient is in fact only 0.25). The reason for a higher correlation with speed is the different way cruising and coasting are accounted for: they are characterized by low current intensity, large distortion and a moderate to high speed (that numerically is more relevant).

The correlation is calculated again for a different case, the French 50 Hz system, and results shown in Table 4 to 6.

Table 4 Correlation coefficient of P_h with I_1 and speed s (French 50 Hz system)

Harm.	$\rho(I_1)$	$\rho_{LB}(I_1)$	$\rho_{UB}(I_1)$	$\rho(s)$	$\rho_{LB}(s)$	$\rho_{UB}(s)$
2	-0.006	-0.036	0.025	-0.023	-0.053	0.007
3	0.286	0.258	0.313	0.025	-0.005	0.055
5	-0.256	-0.2834	-0.227	-0.292	-0.320	-0.265
7	0.342	0.3151	0.368	0.237	0.209	0.266
9	0.322	0.2951	0.349	0.204	0.175	0.233
11	0.073	0.0433	0.103	0.045	0.015	0.075
13	-0.115	-0.1445	-0.085	-0.036	-0.066	-0.006
15	-0.171	-0.2003	-0.142	-0.090	-0.120	-0.060
17	-0.080	-0.1095	-0.050	-0.112	-0.142	-0.083
19	0.026	-0.0039	0.056	0.019	-0.011	0.049
21	0.063	0.0328	0.093	0.122	0.093	0.152
45	-0.023	-0.0528	0.007	0.005	-0.025	0.035
47	-0.035	-0.0644	-0.004	-0.054	-0.084	-0.024
49	-0.154	-0.1829	-0.124	-0.147	-0.176	-0.118
51	-0.010	-0.0401	0.020	-0.064	-0.094	-0.034
53	0.089	0.0588	0.118	0.084	0.054	0.114
55	-0.019	-0.0489	0.011	0.062	0.032	0.092
97	0.107	0.0773	0.137	0.054	0.024	0.084

Table 5 Correlation coefficient of Q_h with I_1 and speed s (French 50 Hz system)

Harm.	$\rho(I_1)$	$\rho_{LB}(I_1)$	$\rho_{UB}(I_1)$	$\rho(s)$	$\rho_{LB}(s)$	$\rho_{UB}(s)$
2	0.0093	-0.0207	0.0393	-0.0245	-0.0545	0.0056
3	0.4498	0.4255	0.4735	0.2675	0.2394	0.2952
5	0.2983	0.2707	0.3254	0.2236	0.1949	0.252
7	0.0006	-0.0294	0.0306	0.0112	-0.0188	0.0412
9	0.0282	-0.0018	0.0582	0.0092	-0.0208	0.0392
11	-0.0027	-0.0327	0.0274	-0.0672	-0.097	-0.0372
13	-0.0022	-0.0322	0.0278	-0.0604	-0.0903	-0.0305
15	0.0237	-0.0064	0.0537	0.0177	-0.0124	0.0477
17	-0.0227	-0.0527	0.0074	0.0198	-0.0103	0.0498
19	-0.0288	-0.0588	0.0012	-0.0351	-0.065	-0.005
21	-0.0021	-0.0321	0.028	-0.082	-0.1117	-0.052
45	0.0942	0.0643	0.1238	0.0823	0.0524	0.112
47	0.0035	-0.0266	0.0335	-0.0385	-0.0684	-0.0085
49	-0.0396	-0.0695	-0.0095	-0.0858	-0.1155	-0.0559
51	-0.0745	-0.1043	-0.0446	-0.1915	-0.2203	-0.1624
53	0.0252	-0.0048	0.0552	-0.049	-0.0789	-0.019
55	0.0522	0.0222	0.0821	0.047	0.017	0.0769
97	0.1152	0.0855	0.1448	0.1055	0.0757	0.1351

It is evident that the harmonic power terms are poorly correlated with the o.c., with only low-order harmonics up to the 9th showing significant values. The nonactive power N_t is significantly correlated to the fundamental I_1 as expected, but scarcely correlated to the speed, simply because the French run was characterized by a substantially high speed with limited braking and traction phases (high-speed train).

Table 6 Correlation coefficient of N_t with I_1 and speed s (French 50 Hz system)

$\rho(\lvert I_1\rvert)$	$\rho_{LB}(\lvert I_1\rvert)$	$\rho_{UB}(\lvert I_1\rvert)$	$\rho(s)$	$\rho_{LB}(s)$	$\rho_{UB}(s)$
0.309	0.281	0.336	0.099	0.069	0.129

It is in general understood that straightforward correlation has the drawback of being influenced by numeric values and that two different systems are thus hardly comparable. In reality, correlation and similarity operated on normalized quantities, such as the sign of P_h, $\underline{P}_h$, are more effective.

5.3. Harmonic power displacement factor

The pair P_h-Q_h corresponds to the harmonic displacement factor d_h, but bears information of intensity, and thus of relevance. It is displayed at various characteristic harmonics during selected t.i. of traction, braking and coasting o.c.. Results are shown in the following figures: Fig. 6 to Fig. 11 for the 16.7 Hz systems, Fig. 12 to Fig. 14 for the 50 Hz system. As anticipated, the harmonic reactive power Q_h originate from common terms to V_h and I_h.

The P_h-Q_h plots lend themselves to the application of clustering techniques, to assess the level of coherence between sets of samples belonging to the same o.c. In this analysis clusters are displayed with different colours and their characteristics are visually assessed for simplicity.

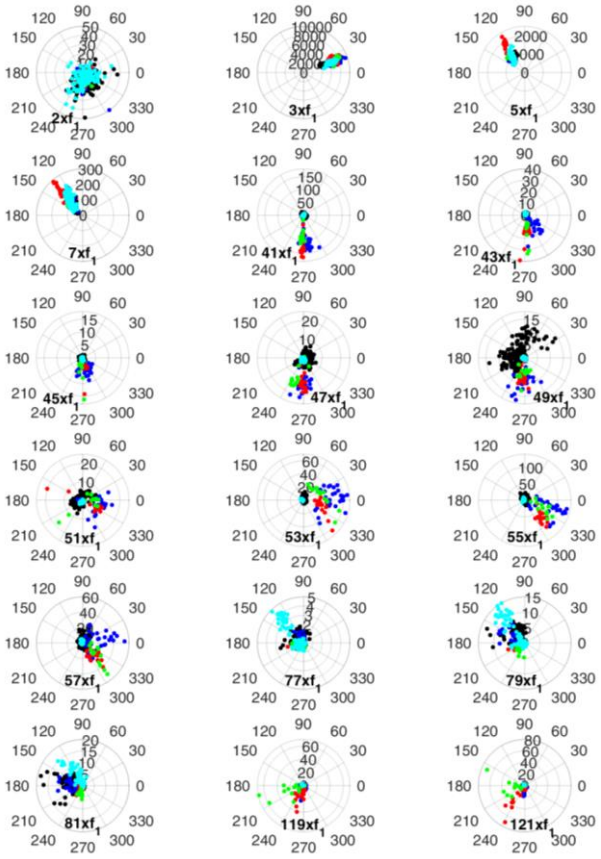

Fig. 6. P_h-Q_h polar diagram for CH 16.7 Hz harmonics: traction condition, five different time intervals (colour).

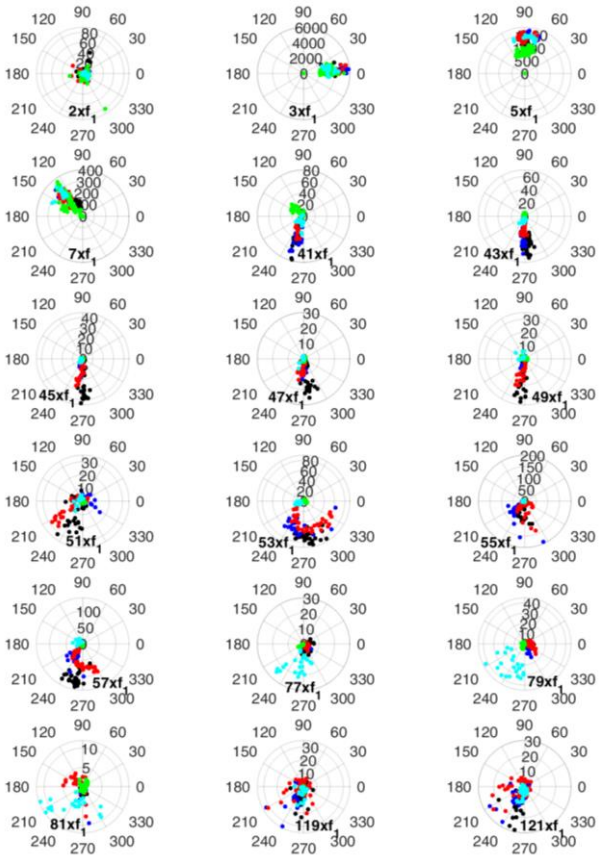

Fig. 7. P_h-Q_h polar diagram for CH 16.7 Hz harmonics: braking condition, five different time intervals (colour).

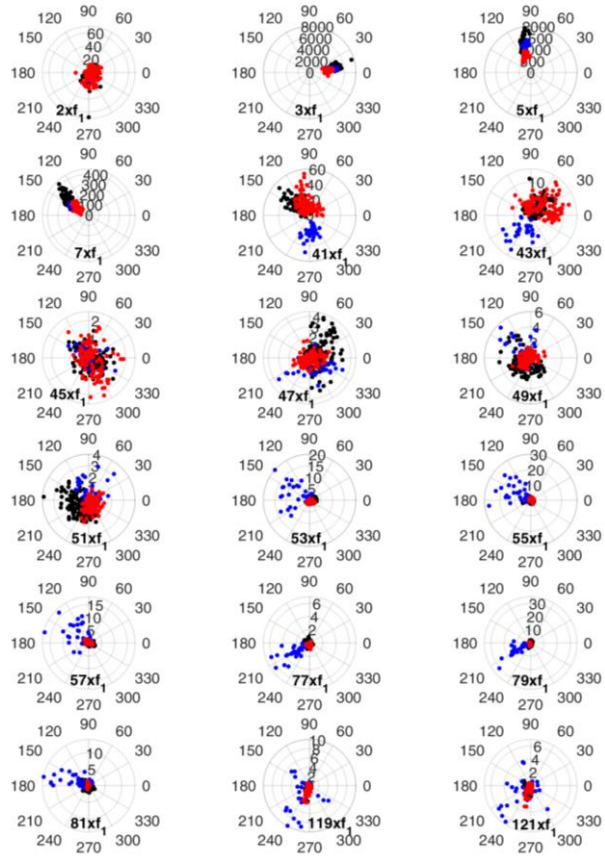

Fig. 8. P_h-Q_h polar diagram for CH 16.7 Hz harmonics: coasting condition, three different time intervals (colour).

Fig. 9. P_h-Q_h polar diagram for D 16.7 Hz harmonics: traction condition, six different time intervals (colour).

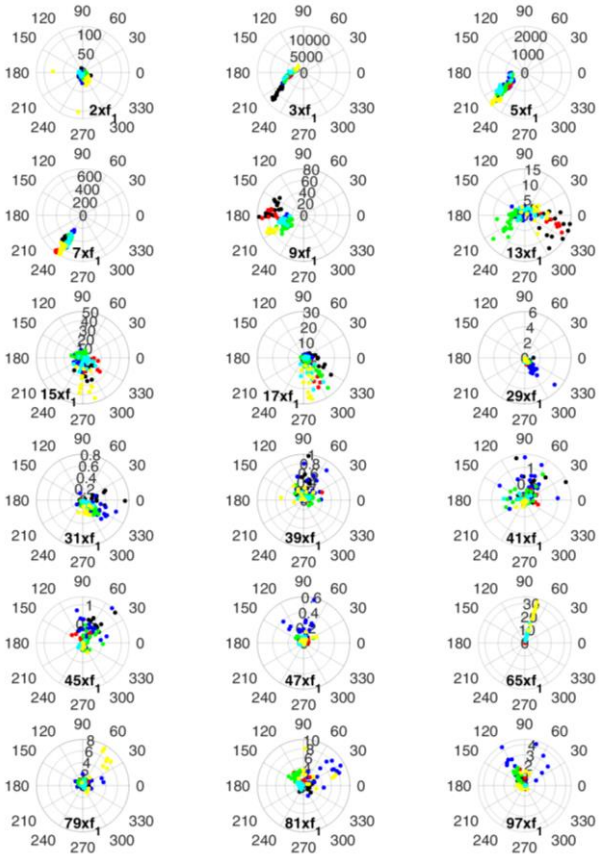

Fig. 10. P_h-Q_h polar diagram for D 16.7 Hz harmonics: braking condition, six different time intervals (colour).

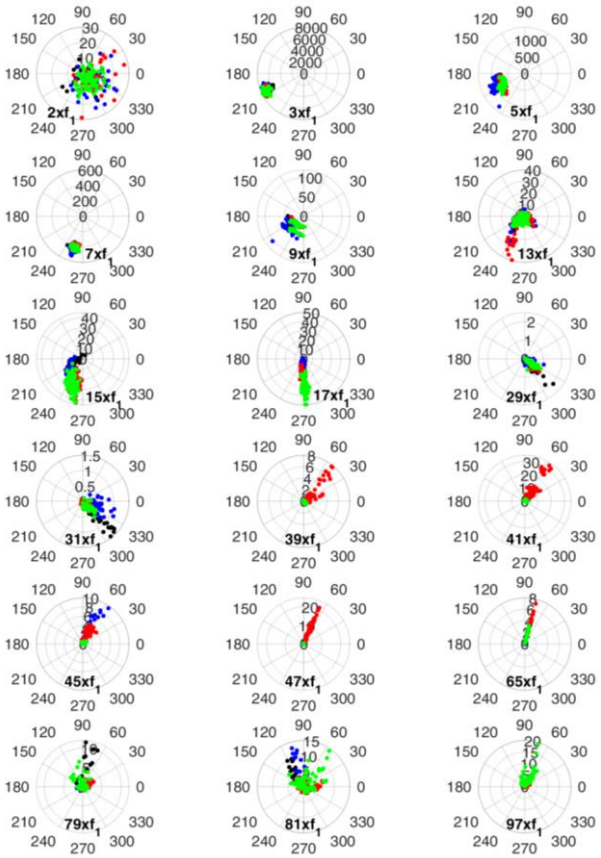

Fig. 11. P_h-Q_h polar diagram for D 16.7 Hz harmonics: coasting condition, four different time intervals (colour).

For both 16.7 Hz systems the 2nd harm. is confirmed not correlated as it has an almost circular shape, quite similar for the three o.c. For Switzerland the 5th and 7th have similar distribution for the various intervals and the three o.c. These three components are related to network distortion originating from the substation, since if caused by other rolling stock they would not be stationary. For Germany the 5th and 7th are coherent for braking and coasting, but show a significant dispersion (especially the 5th) during traction.

For the 3rd harm. the intervals for the same o.c. are in strong agreement, but different o.c. have a consistently different behaviour, although the change of angle and amplitude are not dramatic: a significant portion of the 3rd harm. is due to the auxiliaries, whose operation is almost independent on the traction conditions.

For Switzerland the 51st to 57th show a consistent change of angle passing from traction to braking with the P_h part passing from positive to negative, although there is prevalence of Q_h. Passing to coasting the components are all of negligible amplitude. Similarly the 41st to 47th harm. keep an almost unchanged distribution passing from traction to braking, but spread consistently and reduce their amplitude when in coasting.

For Germany 45th, 47th and 65th components show a consistent correlation, with a constant displacement angle and limited spread, slightly larger for braking o.c.

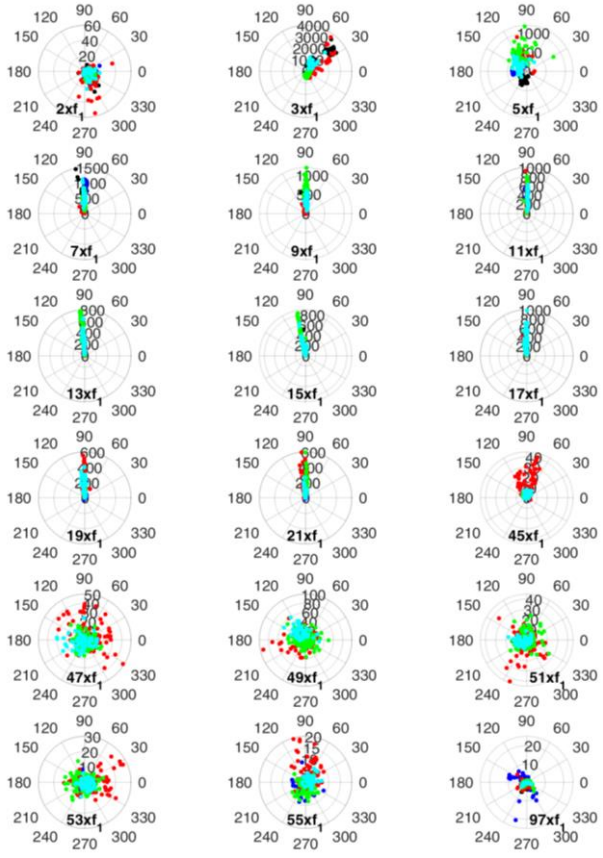

Fig. 12. P_h-Q_h polar diagram for F 50 Hz harmonics: traction condition, five different time intervals (colour).

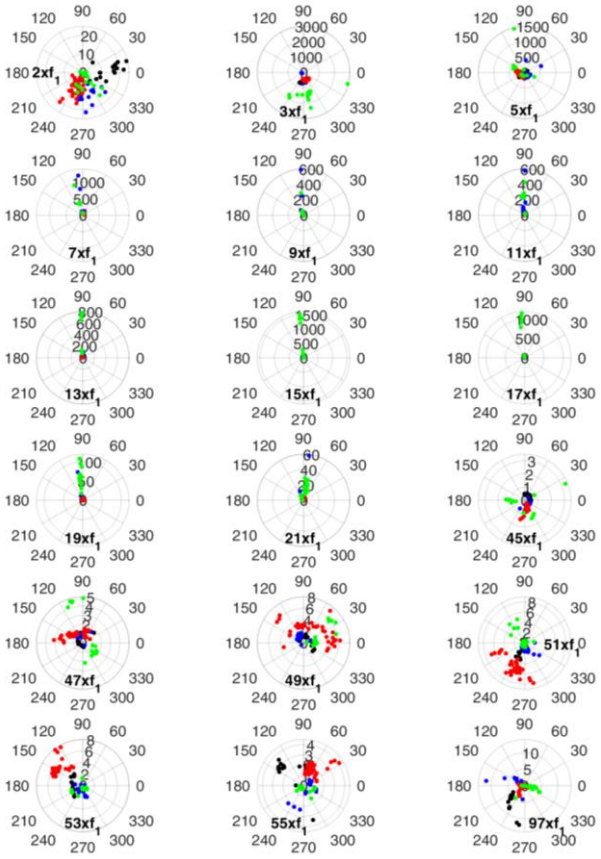

Fig. 13. P_h-Q_h polar diagram for F 50 Hz harmonics: braking condition, four different time intervals (colour).

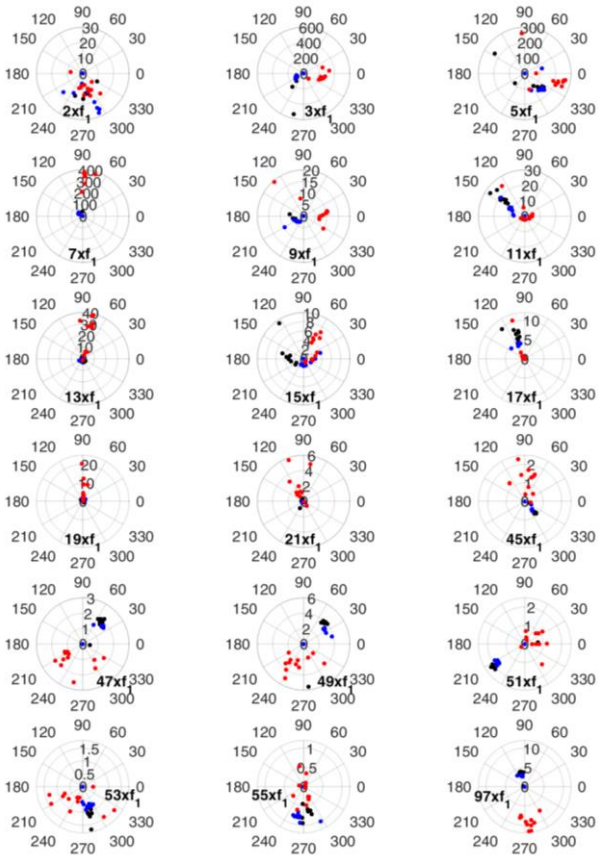

Fig. 14. P_h-Q_h polar diagram for F 50 Hz harmonics: coasting condition, three different time intervals (colour).

For the 50 Hz system considered in Fig. 12 to Fig. 14 there is a significant compactness for P_h-Q_h values of harmonics between 9th and 21st: values are almost overlapped for different time intervals in the same o.c. (traction and braking) and also between o.c. When considering coasting the values are only slightly more dispersed and one or two orders of magnitude smaller, demonstrating that these components are related to the 4QC; if they were caused by the substation and network they would not depend on the o.c. and should be uniformly distributed among the o.c. of the observed train, if the origin were other rolling stock they would depend on other o.c. uncorrelated from those of the observed train.

For the 97th harm there is a significant dispersion between o.c. and between t.i., although within the same time interval values are sufficiently compact. The values are all quite small and similar between o.c..

For harmonics between 45th and 55th the values show a large dispersion again not correlated to o.c. and also within the same time interval; intensity is not much different between o.c., although there is a substantial presence of larger values for traction o.c..

6. Conclusion

Pantograph voltage and current recordings were post processed to calculate harmonic power terms (active, reactive and nonactive power) and to analyze their statistical behavior, correlating active and nonactive harmonic power terms to traction effort and speed, selected as high-level indicators of rolling stock operating conditions. Active and reactive harmonic power values are also analyzed using graphical representations, showing the spread of values among different locations along the line and different operating conditions: clustering and similarity of patterns are exploited to recognize common behavior and correlation, more straightforwardly than a full numeric approach.

The approach was verified with three long recordings of pantograph voltage and current measured in Switzerland and Germany for 15 kV 16.7 Hz supply and France for 2x25 kV 50 Hz supply. Several time intervals were extracted where operating conditions (effort and speed) were almost constant and results compared between similar operating conditions and between systems.

The identified characteristics for the power terms at the low-order harmonics and for those related to converter commutation at higher orders are repeatable and represent a first set of rules. The development of this work is towards a more quantitative assessment of spread and similarity of graphical patterns and the verification of consistency with much larger datasets and different rolling stock, including more modern technologies.

7. References

[1] Emanuel A.E. and Wang X., 'Estimation of Loss of Life of Power Transformers Supplying Nonlinear Loads', IEEE Trans. Power App. and Sys., 1985, 104, (3), pp. 628-636

[2] Said D.M., Nor K.M. and Majid M.S., 'Analysis of Distribution Transformer Losses and Life Expectancy using Measured Harmonic Data', Proc. of 14th Intern. Conf. on Harm. and Quality of Power (ICHQP), Bergamo, Italy, Sept. 26-29, 2010.

[3] Mariscotti A., 'Characterization of Active Power Flow at Harmonics for AC and DC Railway Vehicles', Proc. IEEE Veh. Pow. and Prop. Conf., Hanoi, Vietnam, Oct. 14-17, 2019.
[4] Mariscotti A., 'Relevance of Harmonic Active Power Terms for Energy Consumption in Some Railway Systems', Proc. 23rd IMEKO TC4 Intern. Symp., Xi'an, China, Sept. 17-20, 2017.
[5] Mariscotti A., 'Behaviour of Spectral Active Power Terms for the Swiss 15 kV 16.7 Hz Railway System', Proc. 10th IEEE Intern. Workshop on Applied Meas. for Pow. Systems, Aachen, Germany, Sept. 25-27, 2019.
[6] Lee K.D., Leeb S.B., Norford L.K., Armstrong P.R., Holloway J. and Shaw S.R., 'Estimation of Variable-Speed-Drive Power Consumption from Harmonic Content', IEEE Trans. on Energy Conv., 2005, 20, (3), pp. 566-574
[7] Mirchevski S., Vidanovski D., Rozanov Y. and Ryvkin S., 'Significance of Non-Active Power in Energy Efficiency of Electric Drives', X Intern. Conf. on Electrical Pow. Drive Sys. (ICEPDS), Novocherkassk, Russia, Oct. 3-6, 2018.
[8] Chang G.W., Lin H.-W. and Chen S.-K., 'Modeling Characteristics of Harmonic Currents Generated by High-Speed Railway Traction Drive Converters', IEEE Trans. Pow. Del., 2004, 19, (2), pp. 766-773
[9] Brenna M., Foiadelli F., Roscia M. and Zaninelli D., 'Current Distortion Evaluation in Traction 4Q Constant Switching Frequency Converters', J. Electrom. Analysis & Applications, 2009, 3, pp. 129-137
[10] Agamloh E. B., 'Power and Efficiency Measurement of Motor-Variable-Frequency Drive Systems', IEEE Trans. Industry App., 2017, 53, (1), pp. 766-773
[11] Mariscotti A., Ruscelli M. and Vanti M., 'Modeling of Audiofrequency Track Circuits for validation, tuning and conducted interference prediction', IEEE Trans. Intel. Transp. Sys., 2010, 11, (1), pp. 52-60.
[12] Dolara A, Gualdoni M. and Leva S., 'EMC Disturbances on Track Circuits in the 2×25kV High Speed AC Railways Systems', IEEE Trondheim PowerTech, Trondheim, Norway, June 19-23, 2011.
[13] EN 50463-2: 'Railway applications – Energy measurement on board trains', 2017.
[14] Richter M., Komarnicki P. and Hauer I., 'Improving state estimation in smart distribution grid using synchrophasor technology: a comparison study', Archives of Elec. Eng., 2018, 67, (3), pp. 469-483.
[15] Pegoraro P. A. et al., 'Line Impedance Estimation Based on Synchrophasor Measurements for Power Distribution Systems', IEEE Trans. on Instr. and Meas., 2019, 68, (4), pp. 1002-1013
[16] Frey D., Schanen J., Quintana S., Bollen M. and Conrath C., 'Study of high frequency harmonics propagation in industrial networks', Proc. IEEE Intern. Symp. Electrom. Comp., Rome, Italy, 2012, pp. 1-5.
[17] Rönnberg S. K. et al., 'On waveform distortion in the frequency range of 2-150 kHz – Review and research challenges', Electric Pow. Sys. Res., 2017, 150, pp. 1-10
[18] Mariscotti A., 'Voltage coupled to wayside interconnecting cables', Proc. Intern. Conf. on Elec. Sys. for Aircraft, Railway and Ship Prop. (ESARS), Bologna, Italy, Oct. 21-23, 2010.
[19] Brenna M. et al., 'Investigation of resonance phenomena in high speed railway supply systems: Theoretical and experimental analysis', Elec. Pow. Sys. Res., 2011, 81, pp. 1915-1923
[20] Zhang J., Shang J., and Zhang Z., 'Optimization and Control on High Frequency Resonance of Train-Network Coupling Systems', Math. Problems in Eng., 2019, Article ID 2190452, pp. 1-10
[21] Hemmer B., Mariscotti A. and Wuergler D., 'Recommendations for the calculation of the total disturbing return current from electric traction vehicles', IEEE Trans. on Pow. Del., 2004, 19, (2), pp. 1190-1197
[22] Mariscotti A., 'Data sets of measured pantograph voltage and current of European AC railways', Data In Brief, in print
[23] IEEE Std. 1459: 'IEEE Standard Definitions for the Measurement of Electric Power Quantities under Sinusoidal, Nonsinusoidal, Balanced, or Unbalanced Condition', 2010
[24] Barbaro P.V., Cataliotti A., Cosentino V. and Nuccio S., 'A Novel Approach Based on Nonactive Power for the Identification of Disturbing Loads in Power Systems', IEEE Trans. on Pow. Del., 2007, 22, (3), pp. 1782-1789
[25] Mariscotti A., 'Behavior of Single-Point Harmonic Producer Indicators in Electrified AC Railways', Metrology and Measurement Systems, in print
[26] EN 50388: 'Railway Applications – Power supply and rolling stock – Technical criteria for the coordination between power supply (substation) and rolling stock to achieve interoperability', 2013.
[27] prEN 50388-1: 'Railway Applications – Fixed installations and rolling stock – Technical criteria for the coordination between traction power supply and rolling stock to achieve interoperability – Part 1: General', 2017.
[28] Boschetti G. and Mariscotti A., 'Integrated Electromechanical Simulation of Traction Systems: Relevant Factors for the Analysis and Estimation of Energy Efficiency', Proc. Intern. Conf. on Elec. Sys. for Aircraft, Railway and Ship Prop. (ESARS), Bologna, Italy, Oct. 16-18, 2012.
[29] Bigharaz, M. H. et al., 'A comprehensive simulator of AC autotransformer electrified traction system', Int. J. of Power and Energy Conv., 2019, 10, (2), pp. 129-147.
[30] Mariscotti A., 'Results on the Power Quality of French and Italian 2x25 kV 50 Hz railways', Proc. IEEE Intern. Instrum. and Meas. Techn. Conf. I2MTC, Graz, Austria, May 13-16, 2012
[31]